

# Sequential activation of individual caspases, and of alterations in Bcl-2 proapoptotic signals in a mouse model of Huntington's disease

Yu Zhang,\* Victor O. Ona,\* Mingwei Li,\* Martin Drozda,\* Michel Dubois-Dauphin,† Serge Przedborski,‡ Robert J. Ferrante and Robert M. Friedlander§,¶\*

\*Neuroapoptosis Laboratory, Department of Neurosurgery, Brigham and Women's Hospital, Harvard Medical School, Boston, Massachusetts, USA

†Hôpitaux Universitaires de Genève, Division of Neuropsychiatry, Geneva, Switzerland

‡Department of Neurology and Pathology, Columbia University, New York, USA

§Geriatric Research Education and Clinical Center, Bedford VA Medical Center, Bedford, Massachusetts and Boston University School of Medicine, Boston, Massachusetts, USA

¶Departments of Neurology, Pathology, and Psychiatry, Boston University School of Medicine, Boston, Massachusetts, USA

## Abstract

Caspases play an important role in neurodegeneration in Huntington's disease (HD). Members of the Bcl-2 family are critical modulators of terminal cell death pathways. However, alterations of Bcl-2 family members and their functional role in an *in vivo* model of HD have not been documented. With the goal of gaining mechanistic insight, we used a transgenic mouse model of HD (R6/2) to investigate the chronology of caspase activation and functional alterations in members of the Bcl-2 family. In R6/2 mice caspase activation precedes proapoptotic changes in Bcl-2 family members. Of the caspases that we screened, caspase-1-like activation was the first

to be detected in the disease process (7 weeks). Proapoptotic changes in members of the Bcl-2 family were first detected at 9 weeks. To demonstrate a potential functional/therapeutic role of Bcl-2 in HD, we crossed R6/2 mice with mice overexpressing Bcl-2 in neurons. Transgenic expression of Bcl-2 in R6/2 mice resulted in slight prolonged survival. Understanding the chronology of apoptotic events provides important information for appropriate therapeutic targeting in this devastating and untreatable disease.

**Keywords:** Bcl-2, caspase, Huntington's disease, transgenic mice.

*J. Neurochem.* (2003) **87**, 1184–1192.

Huntington's disease (HD) is a progressive, universally fatal, neurodegenerative disease. HD is caused by a mutation consisting of an expanded CAG repeat in the huntingtin gene (Huntington's Disease Collaborative Research Group 1993). Selective cell death of striatal medium spiny and cortical neurons has been demonstrated in the brains of patients with HD (Ferrante *et al.* 1991). We previously demonstrated a functional role for caspase cell death pathways in HD and other neurologic diseases (Ona *et al.* 1999; Chen *et al.* 2000; Li *et al.* 2000a, 2000b). Caspases, a mammalian family of cysteine proteases with aspartic acid specificity are key mediators of the apoptotic cell-death program (Fraser and Evan 1996; Yuan *et al.* 1993; Martin and Green 1995; Nicholson *et al.* 1995; Tewari *et al.* 1995). In addition to caspases, members of the Bcl-2 family are critical in

modulating the execution of cell death pathways (Boise *et al.* 1993; Kroemer 1997; Adams and Cory 1998). A role for Bcl-2 family members, if any, in HD is not yet clear.

Received June 26, 2003; revised manuscript received August 13, 2003; accepted August 14, 2003.

Address correspondence and reprint requests to Robert M. Friedlander, Department of Neurosurgery, Brigham and Women's Hospital/Harvard Medical School, 221 Longwood Avenue, LMRC 123, Boston, MA 02115, USA. E-mail: rfriedlander@rics.bwh.harvard.edu

*Abbreviations used:* AIF, apoptosis-inducing factor; BH, Bcl-2 homology domain; HD, Huntington's disease; PBS, phosphate-buffered saline; PMSF, phenylmethylsulphonyl fluoride; PVDF, polyvinylidene difluoride; SDS-PAGE, sodium dodecyl sulfate polyacrylamide gel electrophoresis; TUNEL, terminal deoxy nucleotidyl transferase-mediated dUTP biotin nick-end labelling.

Even though they share sequence similarities at conserved Bcl-2 homology domains (BH), Bcl-2 family members are divided into two distinctly opposite functional groups, proapoptotic and antiapoptotic (Adams and Cory 1998; Green and Reed 1998). Antiapoptotic members of the Bcl-2 family include Bcl-2 and Bcl-X<sub>L</sub>. Proapoptotic members of the Bcl-2 family members are further divided into two subfamilies, the Bax subfamily (including Bax and Bak) and the BH3-only subfamily (including Bad, Bid, and Bim). The main determinant of cell fate, as regulated by the Bcl-2 family, is the balance of proapoptotic and antiapoptotic Bcl-2 family members. Regulation of Bcl-2 family signals occurs at the transcriptional (Bim) level (Putcha *et al.* 2001), by subcellular localization (Bax and Bak; Antonsson *et al.* 2001; Nechushtan *et al.* 2001), post-translational modification by cleavage (Bid; Li *et al.* 1998; Luo *et al.* 1998), and phosphorylation/dephosphorylation (Bad; Zha *et al.* 1996).

Mitochondria are in a pivotal site to facilitate the communication between Bcl-2 family members and caspase family members. The Bcl-2 family members are targeted to the mitochondrial membrane by their C-terminal anchor domain or by binding to other members having the anchor domain. Mitochondria play a critical role in cell death by releasing apoptogenic factors such as cytochrome *c*, apoptosis-inducing factor (AIF), Smac/Diablo, Omi/HtrA2, and endonuclease G from the intermembrane space into the cytoplasm (Li *et al.* 1997, 2001; Susin *et al.* 1999; Du *et al.* 2000; Suzuki *et al.* 2001). Cytochrome *c* released from the mitochondria binds to Apaf-1 activating caspase-9, which thereafter results in caspase-3 activation (Li *et al.* 1997; Zou *et al.* 1997). Caspase-3 mediates many of the terminal cell death events. In response to different apoptotic signals, members of the three Bcl-2 subfamilies regulate the release of cytochrome *c* into the cytoplasm and therefore play a key role in modulating downstream caspase activation and cell death by different modification and activation mechanisms.

Caspase-1, -3, and -9 activation has been demonstrated in end-stage HD mouse and human brain specimens (Ona *et al.* 1999; Chen *et al.* 2000; Kiechle *et al.* 2002); activation of caspase-8 has been demonstrated in human HD brain samples (Sanchez *et al.* 1999). However, their temporal course of activation has not been described. Using a transgenic mouse model of HD, we demonstrate that there is an orchestrated timeframe of activation of caspase and proapoptotic alterations of Bcl-2 family members. To evaluate the role of Bcl-2 family members in disease progression, we then crossed HD mice with transgenic mice that overexpress Bcl-2 (NSE-Bcl-2; Dubois-Dauphin *et al.* 1994). Understanding the chronology and interaction of these two key cell death pathways provides important information on the mechanisms of disease progression and should assist

in the development of disease stage-specific rational/targeted therapeutics.

## Materials and methods

### Animals

R6/2 (B6CBA-TgN(HDexon1)62Gpb) mice were obtained from Jackson Laboratory (Bar Harbor, ME, USA), and the colony was maintained in our animal facility. Transgenic mice carrying > 16 copies of human Bcl-2 gene (NSE-Bcl-2) were generated by Dubois-Dauphin *et al.* (1994) and were back-crossed more than five times with B6CBA mice in our lab. Male R6/2 mice were crossed with female Bcl-2 transgenic mice to produce double transgenic R6/2-Bcl-2 and the littermates R6/2-wild-type as controls. Mice were genotyped on post-natal day 14 (Mangiarini *et al.* 1996; Kostic *et al.* 1997). Disease onset and RotaRod performance was tested and scored as described previously (Ona *et al.* 1999). All animal procedures were conducted in accordance with protocols approved by the Harvard Medical School Animal Care Committee.

### Caspase activity assay

A protocol provided by Chemicon for caspase-1-like (YVAD-AFC), caspase-3-like (DEVD-AFC), caspase-8-like (IETD-AFC), and caspase-9-like (LEHD-AFC) fluorometric protease assay kit was used to assay caspase activity. In brief, hemisected fresh (not frozen) brains were homogenized in lysis buffer (Chemicon, kit for caspase fluorometric protease assay) for 10 min. The brain lysate (standardized to protein concentration) was incubated with an equal volume of 2 × reaction buffer (with 0.01 M dithiothreitol) for an additional 1 h at 37°C with caspase-1, 3, 8, and 9 substrates (YVAD-AFC, DEVD-AFC, IETD-AFC, LEHD-AFC) at a final concentration of 50 μM. The fluorescence was measured by a VersaFluor Fluorometer (Bio-Rad, Hercules, CA, USA) with an excitation filter of 390 ± 22 nm and an emission filter of 510 ± 10 nm.

### Immunofluorescence staining

As previously described (Li *et al.* 2000a, 2000b), mice were anesthetized and perfused intracardially with 200 mL phosphate-buffered saline (PBS), PH 7.4 and followed with 200 mL 4% paraformaldehyde in PBS. Brains were frozen in cold isopentane after cryoprotection in 30% sucrose. Frozen sections (10 μm) were washed with PBS containing 0.05% Tween-20 and blocked in 10% normal goat serum for 1 h. P20 (Rat anticaspase-1, generously provided by Dr Yuan; 1 : 3) or CM1 (# 551150, rabbit antiactive caspase-3, BD Pharmingen, San Diego, CA, USA; 1 : 2000) was incubated with sections overnight at 4°C and followed by a 1-h incubation with biotinylated anti-rat or anti-rabbit (1 : 200, Vector Laboratories, Burlingame, CA, USA) at room temperature. Sections were then probed with fluorescein avidin DCS (1 : 1000, Vector Laboratories) for 30 min. After incubation with NeuN (#MAB377B, Chemicon, Temecula, CA, USA; 1 : 100) for 1 h, sections were incubated with Texas Red antibody to mouse (1 : 200, Vector Laboratories) for 30 min and followed with Hoechst 33342 (0.2 μg/mL, Molecular Probes, Eugene, OR, USA) for 20 min. The fluorescent stained sections were evaluated with epifluorescence microscopy.

### Cellular fractionation

Both cytosolic and mitochondrial fractions were extracted from fresh half-brain samples. Tissues were gently homogenized with a Kontes Dounces Tissue Grinder (7 mL capacity) in buffer A (250 mM sucrose, 10 mM KCl, 1.5 mM MgCl<sub>2</sub>, 2 mM EDTA, 20 mM HEPES) with protease inhibitor cocktail set III (Calbiochem, San Diego, CA, USA; Step 1). After being centrifuged at 500 g and 4°C for 5 min, supernatants of homogenates were collected and centrifuged at 13000 g and 4°C for 20 min (Step 2). Resulting pellets were washed once in buffer A and centrifuged at 13000 g and 4°C for 20 min to get the mitochondrial fraction (Step 3). Resulting supernatants from Step 2 were further centrifuged at 100000 g and 4°C for 60 min (Step 4). Supernatants from Step 4 were designated cytosolic fractions. A mouse monoclonal antibody to tubulin (T5168; Sigma, St Louis, MO, USA; 1 : 5000) was used as a loading control and marker for the cytosolic fraction. A mouse monoclonal antibody to COX IV (Clontech, Palo Alto, CA, USA; 1 : 500) was used as a loading control and marker for the mitochondrial fraction.

### Total protein extraction and western blot

Protein was extracted according to the protocol provided by Santa Cruz Biotechnology (Santa Cruz, CA, USA); tissue was homogenized at 4°C in RIPA buffer [1% Nonidet P-40, 0.5% sodium deoxycholate, 0.1% sodium dodecyl sulfate (SDS)] with protease inhibitor cocktail set III (Calbiochem), NaF 1 mM, sodium orthovanadate (1 mM), 10 mM β-glycerophosphate, phenylmethylsulphonyl fluoride (PMSF) (0.1 mg/mL), and 30 μL/mL aprotinin (Sigma). Lysates were centrifuged twice at 10 000 g for 20 min and mixed with an equal volume of 2 × electrophoresis loading buffer [1.0 mL glycerol, 0.5 mL 2-mercaptoethanol, 3.0 mL 10% SDS, 1.25 mL 1.0 M Tris-HCl (pH 6.7) and 1–2 mg bromophenol blue], aliquoted, and stored at –80°C. Protein concentration was assayed by the Bradford dye-binding procedure. Proteins were run in 12% SDS polyacrylamide gel electrophoresis (SDS-PAGE) and transferred electrophoretically to polyvinylidene difluoride (PVDF) membranes. After blocking with 10% milk at room temperature for 2 h, membranes were blotted with the following antibodies: a polyclonal goat antibody to Bid (R&D Systems, Minneapolis, MI, USA; 1 : 1000 in final dilution), a mouse monoclonal antibody to Bax (sc-7480, Santa Cruz Biotechnology; 1 : 1000), a mouse monoclonal antibody to tubulin (T5168; Sigma; 1 : 5000), a mouse monoclonal antibody to cytochrome c (#556433, BD Pharmingen; 1 : 1000), a rabbit polyclonal antibody that detects Bim/Bod (AAP-330; StressGen Biotechnologies, Victoria, Canada; 1 : 1000), a rabbit polyclonal antibody to Bad (#9292; Cell Signal Technology, Beverly, MA, USA; 1 : 1000), a rabbit polyclonal antibody to phospho-Bad (ser112) (#9291; Cell Signal Technology; 1 : 500), a rabbit polyclonal antibody to Bcl-X<sub>L</sub>, and a rabbit polyclonal antibody to Bcl-2 (sc-7195 and sc-783; Santa Cruz Biotechnology; 1 : 1000). Incubation with each of these antibodies, respectively, was followed by a horseradish-conjugated secondary antibody (Amersham Pharmacia Biotech, Piscataway, NJ, USA) and detected with ECL reagents (Amersham Pharmacia Biotech) by exposure to Kodak film.

### Statistical analysis

Data are presented as the mean ± SEM. Statistical comparisons were made by Student's *t*-test.

## Results

### Chronology of caspase activation in R6/2 mice

The R6/2 mouse, a transgenic mouse model of HD, expresses exon-1 of huntingtin with an expanded polyglutamine repeats under the control of its native promoter (Mangiarini *et al.* 1996). To determine the time course of onset of activation of key members of the caspase family, we evaluated brain extracts of R6/2 mice for evidence of caspase-1, -3, -8, and -9 activities. Given its sensitivity and quantitative advantage, a fluorogenic assay was used to evaluate caspase activation. Substrates YVAD-AFC, DEVD-AFC, IETD-AFC and LEHD-AFC were used to evaluate caspase-1-, -3-, -8-, and -9-like activity (Talanian *et al.* 1997; Thornberry *et al.* 1997). Western blots confirming the activation of these particular caspases have already been published. However, most of these studies have focused on late-stage brain specimens. Therefore, to detect earlier and lower magnitude caspase activation fluorogenic assays were evaluated.

Caspase activation was evaluated at different stages of disease progression, including early (7 weeks), middle (9 weeks), and late stages (12 weeks). Disease progression was determined by rotarod performance and weight loss. Degree of caspase activation was determined as the ratio of caspase activity in R6/2 mice to the activity in age-matched wild-type (WT) littermates. Beginning at 7 weeks, caspase-1-like was the earliest caspase activity in R6/2 mice to become activated ( $1.32 \pm 0.11$  vs. WT,  $p = 0.03$ ,  $n = 6$ ; Fig. 1). At 9 weeks (mid-disease progression), caspase-1 like activation was increased and caspase-3-like and caspase-9-like activation could be detected in R6/2 mice (YVAD-AFC,  $1.35 \pm 0.064$  vs. WT,  $p = 0.0089$ ; DEVD-AFC,  $1.66 \pm 0.21$  vs. WT,  $p = 0.031$ ; LEHD-AFC,  $1.27 \pm 0.032$  vs. WT,  $p = 0.0025$ ;  $n = 4$ ). Compared with 9 weeks, caspase-1-like, caspase-3-like, and caspase-9-like activity increased significantly at 12 weeks (YVAD-AFC,  $1.73 \pm 0.147$  vs. WT,  $p = 0.01$ ; DEVD-AFC,  $2.23 \pm 0.28$  vs. WT,  $p = 0.018$ ; LEHD-AFC,  $1.61 \pm 0.169$  vs. WT,  $p = 0.03$ ;  $n = 3$ ). Caspase-8 like activation was only present at 12 weeks of age (IETD-AFC,  $1.37 \pm 0.075$  vs. WT,  $p = 0.02$ ). Therefore, sequential progressive caspase activation is demonstrated, with caspase-1-like activation detected in the early disease stage, caspase-3- and -9-like activation detected in the middle disease stage, and caspase-8-like activation detected in the end stage of the disease.

Using coimmunofluorescence staining techniques, we then evaluated whether caspase-1 and -3 activation was neuronal in nature. NeuN was used to specifically identify neurons. The antibodies used, although they recognize the caspase precursor, they are most specific for the activated form of the enzyme (Li *et al.* 2000a, 2000b). Beginning at 7 weeks and

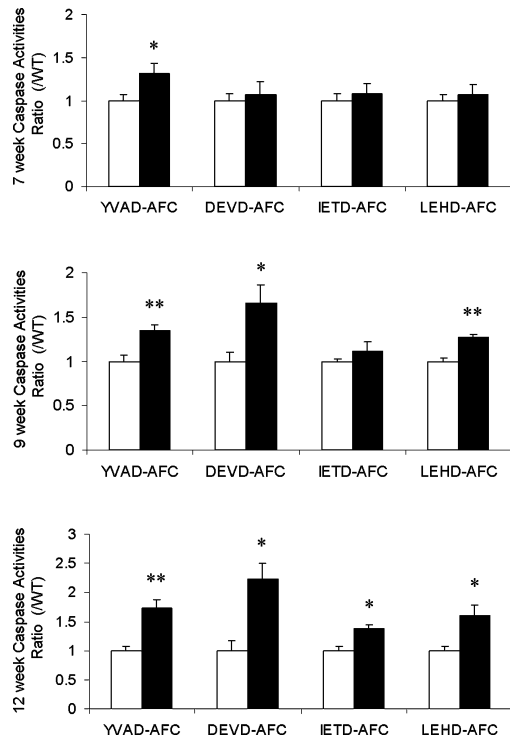


**Fig. 1** Timecourse of caspase activation in brains of R6/2 mice. Caspase activities were detected by a fluorometric protease assay using substrates for caspase-1-like (YVAD-AFC), caspase-3-like (DEVD-AFC), caspase-8-like (IETD-AFC), and caspase-9-like (LEHD-AFC). Data are presented as the ratio of the fluorescence units in R6/2 mice (■) to those in age-matched wild-type mice (□). Concomitant with disease progression, caspases were sequentially and progressively activated. Caspase-1-like activation started at 7 weeks and was the first one activated. Increases in caspase-3-like and caspase-9-like activities were detected starting at 9 weeks. Caspase-8-like activation was not detected until 12 weeks. Error bars indicate SEM ( $n = 6$  in 7 weeks;  $n = 4$  in 9 weeks;  $n = 3$  in 12 weeks; \* $p < 0.05$ ; \*\* $p \leq 0.01$ ).

progressively thereafter, we detect increased caspase immunoreactivity in neurons from R6/2 mice (Fig. 2). No significant caspase-1 or -3 immunoreactivity was detected in the neurons of age-matched WT littermates (Figs 2c, d, k, and l). Caspase staining was associated primarily with NeuN-positive cells, although caspase-positive/NeuN-negative cells were detected. Consistent with the diffuse neuropathology in R6/2 mice, active caspase-positive neurons were present throughout the brain; however, they were most prominent in the striatum and hippocampus (Figs 2g, h, o, and p).

#### Chronology of proapoptotic changes of Bcl-2 family members in R6/2 mice

Parallel with the evaluation of caspase activation at different stages of disease progression, we evaluated Bcl-2 family proteins by western blot analysis in total lysate and, when indicated, in mitochondrial components from R6/2 mouse brains. The evaluated proteins included Bcl-2 and Bcl-X<sub>L</sub> in

the Bcl-2 subfamily; Bax in the Bax subfamily; and Bid, Bad, pBad (phospho-Bad), and Bim in the BH-3-only subfamily. In the early stages of disease progression (6–7 weeks), we did not detect any significant differences in the Bcl-2 family member proteins between the brains of WT and those of R6/2 mice (data not shown). Starting at 9 weeks, there is a decrease in full-length Bid (0.71 vs. WT,  $p < 0.05$ ) associated with an increase in truncated Bid protein (1.2 vs. WT,  $p < 0.01$ ) (Figs 3a and b). Bad, pBad, Bim, and Bax demonstrated no significant difference at 9 weeks (Figs 3a and b). At the late stage of disease (12 weeks), there was a significant increase in Bim (2.62 vs. WT,  $p < 0.05$ ) and a significant decrease in pBad (0.63 vs. WT,  $p < 0.05$ ) (Figs 3c and d) in total lysate. An increase of Bax in the mitochondrial fraction was found in 9- and 12-week-old R6/2 mice (1.38 vs. WT,  $p < 0.05$ ; Figs 4a and b). Increases in Bim in mitochondrial fractions were also found in R6/2 mice at 12 weeks (1.67 vs. WT,  $p < 0.05$ ; Figs 4a and b). No changes of Bcl-2 or Bcl-X<sub>L</sub> were detected either in the total brain lysate or in the mitochondrial/cytosolic fraction (Figs 3 and 4).

#### Overexpression of Bcl-2 slows disease progression in R6/2 mice

The cleavage of Bid, translocation of Bax, increase in Bim, and decrease in pBad, all proapoptotic changes in Bcl-2 family members, were detected in association with disease progression in R6/2 mice. To determine whether balance of Bcl-2 family members plays a role in disease progression in R6/2 mice, we crossed R6/2 mice with transgenic mice selectively overexpressing Bcl-2 in neurons under the control of the neuron-specific enolase promoter (NSE-Bcl-2; Dubois-Dauphin *et al.* 1994; Alberi *et al.* 1996). Unlike other NSE-Bcl-2 transgenic mice, this particular strain of mice does not have an enlarged brain or demonstrate increased neuronal populations. The density of counted neurons in the retina (ganglion cells), hippocampus, and cortex was similar between WT and NSE-Bcl-2 mice (M. Dubois-Dauphin, unpublished data). Bcl-2 transgenic immunoreactivity has been evaluated in the cortex and basal ganglia. In the cortex, neuronal Bcl-2 transgenic overexpression is diffusely detected. In the basal ganglia, Bcl-2 transgenic overexpressing cells are present, but the expression is not generalized to all cells (M. Dubois-Dauphin, unpublished data). Compared with R6/2 mice, double transgenic R6/2-NSE-Bcl-2 littermates demonstrated a statistically significant delay in onset of motor deficits and extended survival (10.3%; Figs 5a, b, and d). Consistent with the magnitude of proapoptotic changes in Bcl-2 family members, the magnitude in the prolongation of survival is smaller than caspase inhibition (20–25%; Ona *et al.* 1999). RotaRod was used to evaluate motor performance and coordination. R6/2-NSE-Bcl-2 mice showed a trend towards better performance than R6/2 mice did. Improved performance was statistically significantly in

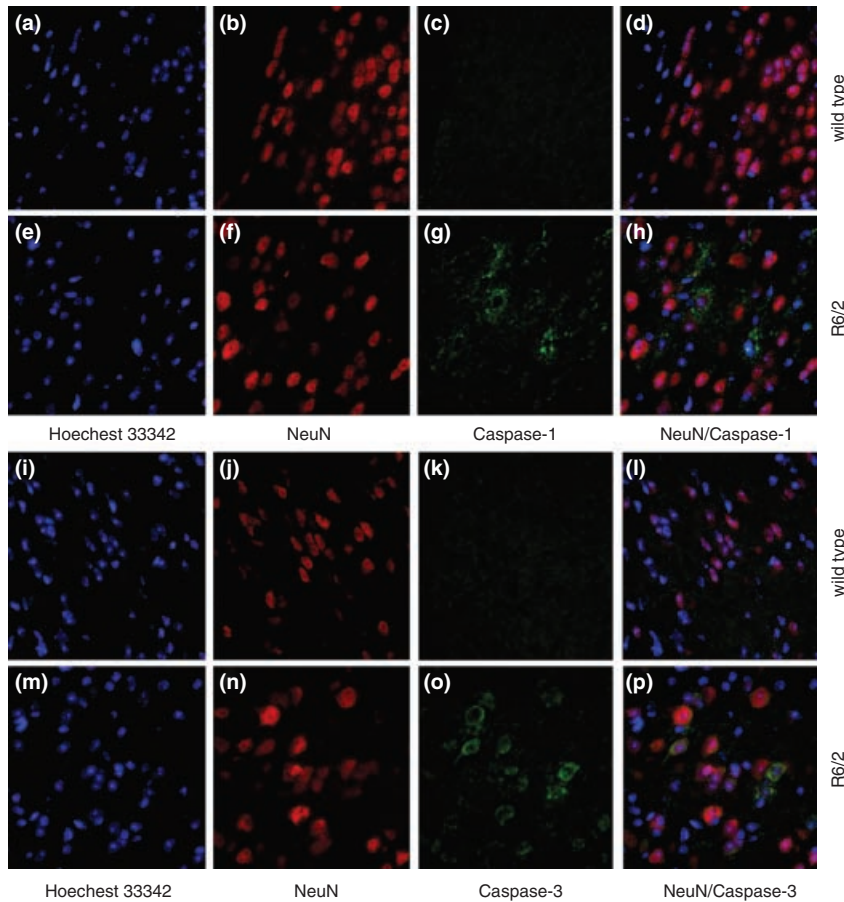


**Fig. 2** Caspase-1 and caspase-3 were detected by immunofluorescence staining in the brains of 12-week-old R6/2 mice and their wild-type littermates. Sections were stained with Hoechst 33342 (d, h, l, and p), NeuN (b, f, j, and n), antibody to caspase-1 (c and g), and antibody to caspase-3 (k and o). Merged images (d from a–c, h from e–g, l from i–k, and p from m–o) demonstrate neuronal immunolocalization of caspase-1 and caspase-3 in brains of R6/2 mice. Caspase-1 and caspase-3 were not detected in brains of wild-type mice by immunofluorescence staining ( $n = 3$  mice per group).

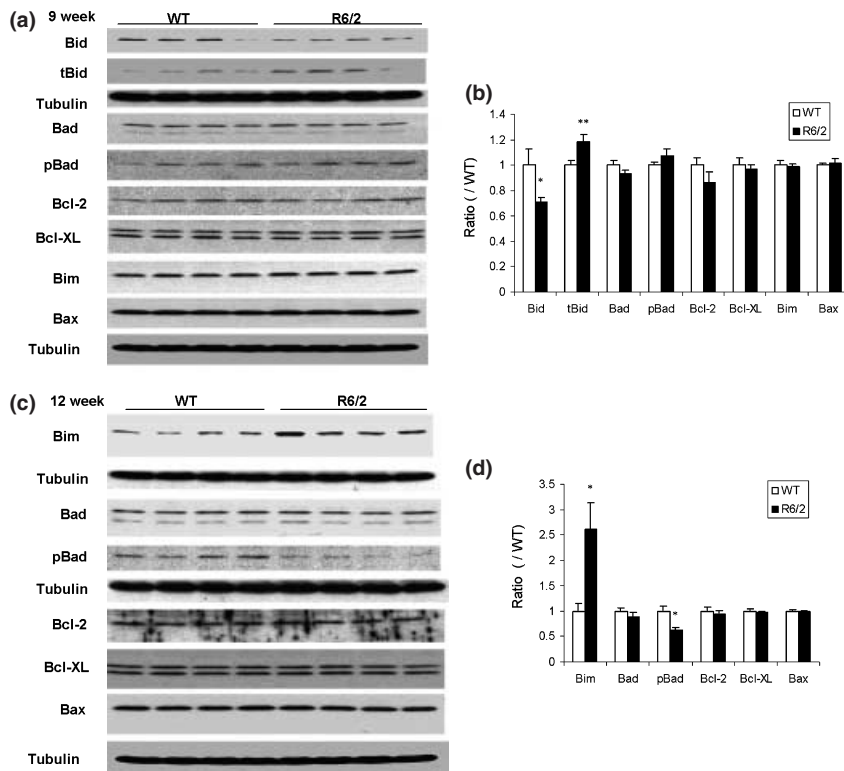


**Fig. 3** Western blot of Bcl-2 family proteins in total brain lysate of R6/2 mice and age-matched wild-type littermates. (a and b) Decreased full-length Bid is associated with increased truncated Bid in 9-week-old R6/2 mice. No significant difference was found in Bcl-2, Bcl-X<sub>L</sub>, Bim, Bad, pBad, and Bax proteins at 9 weeks. Each lane represents a different mouse (a). (c and d) Increased Bim and decreased pBad proteins were found in 12-week-old R6/2 mice. No significant difference was found in Bcl-2, Bcl-X<sub>L</sub>, Bad, and Bax proteins. Each lane represents a different mouse (a and c). Each blot was stripped and reprobbed with antitubulin antibody. Density of each lane was normalized to the corresponding tubulin signal. Each protein was analyzed as the ratio to mean in age-matched wild-type littermate (WT; b and d). Error bars indicate SEM ( $n = 4$ , \* $p < 0.05$ . \*\* $p < 0.01$ ).

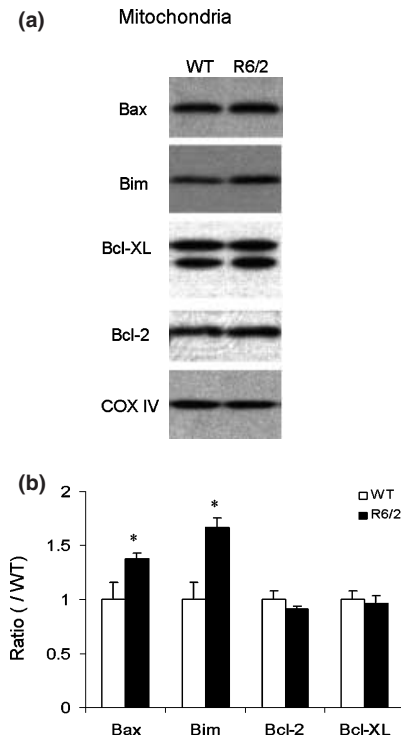


**Fig. 4** Western blot of Bcl-2 family proteins in the mitochondrial fraction of brains of R6/2 mice and age-matched wild-type littermates (a). Increased levels of Bax were detected in mitochondrial fractions of R6/2 mice at 9 and 12 weeks of age (representative band of a 9-week-old mouse). Increased Bim in the mitochondrial fraction was detected at 12 weeks in R6/2 mice. No significant difference was found in levels of Bcl-2 or Bcl-X<sub>L</sub> at both 9 weeks and 12 weeks (representative band of a 12-week-old mouse). Each blot was stripped and reprobbed with COX IV antibody. Density of each lane was normalized to corresponding COX IV signal. Each lane is representative of four animals per group (a). Each protein was analyzed as the ratio to mean in age-matched wild-type littermate (b). Error bars indicate SEM ( $n = 4$ ,  $*p < 0.05$ ).

the double transgenic mice compared with the single transgenic mice at the early stage (6 weeks) and late stage (11 weeks) of the disease (Fig. 5c).

## Discussion

Consistent with our previous report of increased levels of caspase-1 and caspase-3 transcription and activation in end-stage HD transgenic mice, we report here the sequential increase in caspase-1-, -3-, -8-, and -9-like activity at different stages of disease progression in R6/2 mice. We also demonstrate a change in proapoptotic balance of Bcl-2 family members in the middle and late stages of disease progression (Fig. 6), which paralleled the onset of cytochrome *c* release from the mitochondria in R6/2 mice (Kiechle *et al.* 2002). Consistent with these alterations, transgenic overexpression of Bcl-2 results in a delayed onset

of motor deficits and extended survival in R6/2 mice (Fig. 5). These results demonstrate a role of Bcl-2 family members, in addition to a role for caspases, in the pathogenesis of disease progression in R6/2 mice. These findings provide new insights into the mechanisms of neuronal death in a chronic disease setting and suggest new sites of therapeutic intervention in HD.

Cleavage of Bid, translocation of Bax, decrease in pBad, and increase in Bim were changes associated with disease progression in R6/2 mice. Bid previously was demonstrated to be a substrate of caspase-8, caspase-1, calpain, and granzyme B (Li *et al.* 1998; Chen *et al.* 2001). Previous reports have demonstrated that Fas-induced activation of caspase-8 results in cleavage of full-length Bid to a truncated form (tBid; Li *et al.* 1998; Luo *et al.* 1998); C-terminal tBid then translocates to the mitochondrial membrane by interacting with Bcl-X<sub>L</sub> or Bax, ultimately mediating cytochrome *c* release. In our report, Bid was cleaved by 9 weeks. The enzymatic activity of caspase-8 was not detected until 12 weeks, suggesting that caspase-8 is not likely to be involved in the early Bid cleavage. Caspase-1 activation was detected as early as 7 weeks. Thus, caspase-1 may be the protease that contributes to early Bid cleavage, which will lead to the translocation of tBid to the mitochondria, resulting in cytochrome *c* release (Kiechle *et al.* 2002), and thereafter caspase-9 and caspase-3 activation. Transcriptional upregulation of caspase-1 results from nuclear translocation of mutant huntingtin N-terminal fragments (Li *et al.* 2000c). A key link therefore results between the caspase and Bcl-2 family from caspase-1-mediated Bid cleavage. A similar role of caspase-1 in Bid cleavage has been proposed in an ALS transgenic mouse model. Crossing an ALS transgenic mouse (SOD1<sup>G93A</sup>) with a transgenic mouse that expresses a dominant negative mutant (M17Z) of caspase-1 resulted in the almost complete disappearance of cleavage of Bid in early symptomatic SOD1<sup>G93A</sup>/M17Z mice compared with the cleavage in age-matched SOD1<sup>G93A</sup> littermates (Guegan *et al.* 2002). In addition, tBid can be generated by calpains (Chen *et al.* 2001, 2002). Activation of calpain was found in HD patients and rat models of HDs by 3-nitropropionic acid injection (Gafni and Ellerby 2002; Bizat *et al.* 2003; Pang *et al.* 2003). In addition to caspases, calpains appear to play a fundamental role in HD pathogenesis (Gafni and Ellerby 2002; Bizat *et al.* 2003).

Bad and Bim are BH-3-only domain members play an important role in the regulation of cytochrome *c* release. Following exposure to a death stimulus, phosphorylated Bad is dephosphorylated (Zha *et al.* 1996; Datta *et al.* 2000). Our findings in R6/2 mice demonstrate a significant decrease in pBad and an increase in Bim levels during the late stage of disease progression. Both of these proapoptotic changes antagonize the prosurvival action of Bcl-2 and Bcl-X<sub>L</sub>, increasing the release of cytochrome *c*, which in turn results in caspase-9 and -3 activation (Kiechle *et al.* 2002).

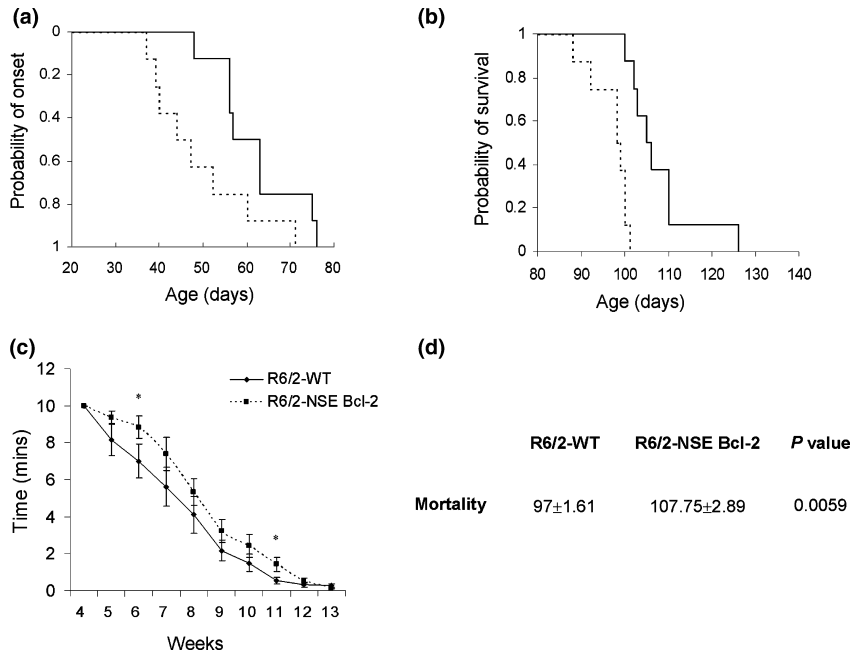


**Fig. 5** Overexpression of Bcl-2 prolonged survival in R6/2 mice. Cumulative probability of onset (a) and survival (b) in R6/2-NSEBcl-2 and R6/2. Solid line, R6/2-NSEBcl-2; dashed line, R6/2-wild-type. Compared with R6/2-wild-type, R6/2-NSE-Bcl-2 demonstrated a delayed onset and a prolonged survival. (c) Mice were evaluated using a Rotarod at 15 rpm (\* $p < 0.05$ ). At the 6-week and 11-week time points, R6/2-NSE-Bcl-2 mice reached a significant improvement in Rotarod performance. (d) Lifespan of double transgenic R6/2-NSE-Bcl-2 mice extended 10.3% longer than R6/2-wild-type littermates ( $n = 8$  per group).

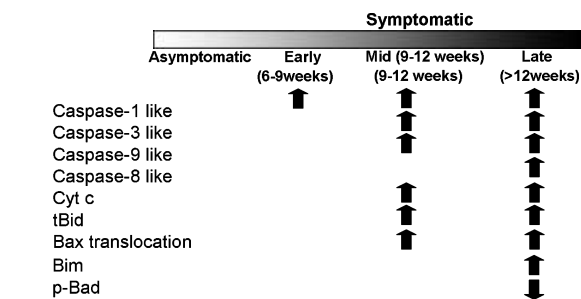


**Fig. 6** Timecourse of caspase activation, of cytochrome *c* release, and of proapoptotic alterations of Bcl-2 family members in R6/2 mice.

The first alteration that we detected was of caspase-1 like activation at 7 weeks of age. At this age, approximately 50% mice have early manifestations of disease onset. Mutant human exon-1 likely mediates an initial toxic gain of function, resulting in cellular toxicity, and disease onset prior to detectable caspase activation. Our data are therefore consistent with a model in which toxicity results from a toxic gain of function of mutant huntingtin. N-terminal mutant huntingtin fragments translocate into the nucleus, resulting in caspase-1 transcriptional upregulation and enzymatic activation (Li *et al.* 2000c). We have previously demonstrated transcriptional upregulation of caspase-1 in R6/2 mice beginning at 7 weeks of age (Chen *et al.* 2000). As disease progresses, caspase-1 cleaves Bid, resulting in release of cytochrome *c* (Kiechle *et al.* 2002), which thereafter binds to Apaf-1, causing caspase-9 and -3 activation.

Compared with acute neurological diseases, the magnitude of caspases activation is much lower in chronic neurodegenerative disease. For example, caspase-1 activation (as

determined by measuring mature IL-1 $\beta$ ) is increased 2.4- to 2.6-fold in experimental models of ALS and HD, compared to 17- to 22-fold in models of ischemia and spinal cord injury (Friedlander *et al.* 1997; Ona *et al.* 1999; Chen *et al.* 2000; Li *et al.* 2000a, 2000b; Friedlander 2003). Therefore, given that the magnitude of caspase activation is different, the cell death process in chronic neurodegenerative disease is different from acute neurological diseases. Although the role of caspase-1 in R6/2 mice disease progression is demonstrated by crossing R6/2 mice with caspase-1 dominant negative (NSE-M17Z) mice, typical apoptotic cell death morphology has not been detected by terminal deoxy nucleotidyl transferase-mediated dUTP biotin nick-end labelling (TUNEL) staining (Turmaine *et al.* 2000; Yu *et al.* 2003). Furthermore, in R6/2 mice, cell dysfunction can be documented by the downregulation of neurotransmitter receptors (Cha 2000). Expression of a caspase-1 dominant negative transgene results in inhibition of the downregulation of these receptors, providing a link between inhibition of caspases and inhibition of cell dysfunction (Ona *et al.* 1999). Therefore it appears that a sublethal magnitude of caspase activation might lead to cell dysfunction and not to cell death in R6/2 mice.

Detailed understanding of the timeframe of events mediating pathogenic changes in chronic neurodegenerative diseases will enable the design of disease stage-sensitive rational/targeted therapeutics for these devastating and often untreatable groups of diseases. Given the differences between the R6/2 mouse and humans with HD, caution must be observed when interpreting these results. On the other hand, these results may provide insight into the

mechanisms not only of HD, but also of other polyglutamine diseases and chronic neurodegenerative diseases.

### Acknowledgements

We thank Nancy Voynow and Jaylyn Olivo at the Brigham and Women's Hospital Editorial Service for editorial assistance. This work was supported by a grant from the Huntington's Disease Society of America (to RMF); the Hereditary Disease Foundation (to RMF); NINDS (to RMF, RJF) and the Veterans Administration (RJF).

### References

- Adams J. M. and Cory S. (1998) The Bcl-2 protein family: arbiters of cell survival. *Science* **281**, 1322–1326.
- Alberi S., Raggenbass M., de Bilbao F. and Dubois-Dauphin M. (1996) Axotomized neonatal motoneurons overexpressing the bcl2 proto-oncogene retain functional electrophysiological properties. *Proc. Natl Acad. Sci. USA* **93**, 3978–3983.
- Antonsson B., Montessuit S., Sanchez B. and Martinou J. C. (2001) Bax is present as a high molecular weight oligomer/complex in the mitochondrial membrane of apoptotic cells. *J. Biol. Chem.* **276**, 11615–11623.
- Bizat N., Hermel J. M., Boyer F. *et al.* (2003) Calpain is a major cell death effector in selective striatal degeneration induced *in vivo* by 3-nitropropionate: implications for Huntington's disease. *J. Neurosci.* **23**, 5020–5030.
- Boise L. H., Gonzalez-Garcia M., Postema C. E. *et al.* (1993) bcl-x, a bcl-2-related gene that functions as a dominant regulator of apoptotic cell death. *Cell* **74**, 597–608.
- Cha J. H. (2000) Transcriptional dysregulation in Huntington's disease. *Trends Neurosci.* **23**, 387–392.
- Chen M., Ona V. O., Li M. *et al.* (2000) Minocycline inhibits caspase-1 and caspase-3 expression and delays mortality in a transgenic mouse model of Huntington disease. *Nat. Med.* **6**, 797–801.
- Chen M., He H., Zhan S., Krajewski S., Reed J. C. and Gottlieb R. A. (2001) Bid is cleaved by calpain to an active fragment *in vitro* and during myocardial ischemia/reperfusion. *J. Biol. Chem.* **276**, 30724–30728.
- Chen M., Won D. J., Krajewski S. and Gottlieb R. A. (2002) Calpain and mitochondria in ischemia/reperfusion injury. *J. Biol. Chem.* **277**, 29181–29186.
- Datta S. R., Katsov A., Hu L., Petros A., Fesik S. W., Yaffe M. B. and Greenberg M. E. (2000) 14-3-3 proteins and survival kinases cooperate to inactivate BAD by BH3 domain phosphorylation. *Mol. Cell* **6**, 41–51.
- Du, C., Fang M., Li Y., Li L. and Wang X. (2000) Smac, a mitochondrial protein that promotes cytochrome *c*-dependent caspase activation by eliminating IAP inhibition. *Cell* **102**, 33–42.
- Dubois-Dauphin M., Frankowski H., Tsujimoto Y., Huarte J. and Martinou J. C. (1994) Neonatal motoneurons overexpressing the bcl-2 protooncogene in transgenic mice are protected from axotomy-induced cell death. *Proc. Natl Acad. Sci. USA* **91**, 3309–3313.
- Ferrante R. J., Kowall N. W. and Richardson E. P. Jr (1991) Proliferative and degenerative changes in striatal spiny neurons in Huntington's disease: a combined study using the section-Golgi method and calbindin D28k immunocytochemistry. *J. Neurosci.* **11**, 3877–3887.
- Fraser A. and Evan G. (1996) A license to kill. *Cell* **85**, 781–784.
- Friedlander R. M. (2003) Apoptosis and caspases in neurodegenerative diseases. *N. Engl. J. Med.* **348**, 1365–1375.
- Friedlander R. M., Gagliardini V., Hara H. *et al.* (1997) Expression of a dominant negative mutant of interleukin-1 beta converting enzyme in transgenic mice prevents neuronal cell death induced by trophic factor withdrawal and ischemic brain injury. *J. Exp. Med.* **185**, 933–940.
- Gafni J. and Ellerby L. M. (2002) Calpain activation in Huntington's disease. *J. Neurosci.* **22**, 4842–4849.
- Green D. R. and Reed J. C. (1998) Mitochondria and apoptosis. *Science* **281**, 1309–1312.
- Guegan C., Vila M., Teissman P., Chen C., Onteniente B., Li M., Friedlander R. and Przedborski S. (2002) Instrumental activation of Bid by caspase-1 in a transgenic mouse model of ALS. *Mol. Cell Neurosci.* **20**, 553.
- Huntington's Disease Collaborative Research Group. (1993) A novel gene containing a trinucleotide repeat that is expanded and unstable on Huntington's disease chromosomes. *Cell* **72**, 971–983.
- Kiechle T., Dedeoglu A., Kubilus J., Kowall N. W., Beal M. F., Friedlander R., Hersch S. M. and Ferrante R. J. (2002) Cytochrome *c* and caspase-9 expression in Huntington's disease. *Neuromol. Med.* **1**, 183–195.
- Kostic V., Jackson-Lewis V., de Bilbao F., Dubois-Dauphin M. and Przedborski S. (1997) Bcl-2: prolonging life in a transgenic mouse model of familial amyotrophic lateral sclerosis. *Science* **277**, 559–562.
- Kroemer G. (1997) The proto-oncogene Bcl-2 and its role in regulating apoptosis. *Nat. Med.* **3**, 614–620.
- Li H., Zhu H., Xu C. J. and Yuan J. (1998) Cleavage of BID by caspase 8 mediates the mitochondrial damage in the Fas pathway of apoptosis. *Cell* **94**, 491–501.
- Li L. Y., Luo X. and Wang X. (2001) Endonuclease G is an apoptotic DNase when released from mitochondria. *Nature* **412**, 95–99.
- Li M., Ona V. O., Chen M., Kaul M., Tenneti L., Zhang X., Stieg P. E., Lipton S. A. and Friedlander R. M. (2000a) Functional role and therapeutic implications of neuronal caspase-1 and -3 in a mouse model of traumatic spinal cord injury. *Neuroscience* **99**, 333–342.
- Li M., Ona V. O., Guegan C. *et al.* (2000b) Functional role of caspase-1 and caspase-3 in an ALS transgenic mouse model. *Science* **288**, 335–339.
- Li P., Nijhawan D., Budihardjo I., Srinivasula S. M., Ahmad M., Alnemri E. S. and Wang X. (1997) Cytochrome *c* and dATP-dependent formation of Apaf-1/caspase-9 complex initiates an apoptotic protease cascade. *Cell* **91**, 479–489.
- Li S. H., Lam S., Cheng A. L. and Li X. J. (2000c) Intracellular huntingtin increases the expression of caspase-1 and induces apoptosis. *Hum. Mol. Genet.* **9**, 2859–2867.
- Luo X., Budihardjo I., Zou H., Slaughter C. and Wang X. (1998) Bid, a Bcl2 interacting protein, mediates cytochrome *c* release from mitochondria in response to activation of cell surface death receptors. *Cell* **94**, 481–490.
- Mangiarini L., Sathasivam K., Seller M. *et al.* (1996) Exon 1 of the HD gene with an expanded CAG repeat is sufficient to cause a progressive neurological phenotype in transgenic mice. *Cell* **87**, 493–506.
- Martin S. J. and Green D. R. (1995) Protease activation during apoptosis: death by a thousand cuts? *Cell* **82**, 349–352.
- Nechushtan A., Smith C. L., Lamensdorf I., Yoon S. H. and Youle R. J. (2001) Bax and Bak coalesce into novel mitochondria-associated clusters during apoptosis. *J. Cell Biol.* **153**, 1265–1276.
- Nicholson D. W., Ali A., Thornberry N. A. *et al.* (1995) Identification and inhibition of the ICE/CED-3 protease necessary for mammalian apoptosis. *Nature* **376**, 37–43.
- Ona V. O., Li M., Vonsattel J. P. *et al.* (1999) Inhibition of caspase-1 slows disease progression in a mouse model of Huntington's disease. *Nature* **399**, 263–267.

- Pang Z., Bondada V., Sengoku T., Siman R. and Geddes J. W. (2003) Calpain facilitates the neuron death induced by 3-nitropropionic acid and contributes to the necrotic morphology. *J. Neuropathol. Exp. Neurol.* **62**, 633–643.
- Putcha G. V., Moulder K. L., Golden J. P., Bouillet P., Adams J. A., Strasser A. and Johnson E. M. (2001) Induction of BIM, a proapoptotic BH3-only BCL-2 family member, is critical for neuronal apoptosis. *Neuron* **29**, 615–628.
- Sanchez I., Xu C. J., Juo P., Kakizaka A., Blenis J. and Yuan J. (1999) Caspase-8 is required for cell death induced by expanded polyglutamine repeats. *Neuron* **22**, 623–633.
- Susin S. A., Lorenzo H. K., Zamzami N. *et al.* (1999) Molecular characterization of mitochondrial apoptosis-inducing factor. *Nature* **397**, 441–446.
- Suzuki Y., Imai Y., Nakayama H., Takahashi K., Takio K. and Takahashi R. (2001) A serine protease, HtrA2, is released from the mitochondria and interacts with XIAP, inducing cell death. *Mol. Cell* **8**, 613–621.
- Talanian R. V., Quinlan C., Trautz S., Hackett M. C., Mankovich J. A., Banach D., Ghayur T., Brady K. D. and Wong W. W. (1997) Substrate specificities of caspase family proteases. *J. Biol. Chem.* **272**, 9677–9682.
- Tewari M., Quan L. T., O'Rourke K., Desnoyers S., Zeng Z., Beidler D. R., Poirier G. G., Salvesen G. S. and Dixit V. M. (1995) Yama/ CPP32 $\beta$ , a mammalian homolog of CED-3, is a CrmA-inhibitable protease that cleaves the death substrate poly-(ADP-ribose) polymerase. *Cell* **81**, 801–809.
- Thornberry N. A., Rano T. A., Peterson E. P. *et al.* (1997) A combinatorial approach defines specificities of members of the caspase family and granzyme B. Functional relationships established for key mediators of apoptosis. *J. Biol. Chem.* **272**, 17907–17911.
- Turmaine M., Raza A., Mahal A., Mangiarini L., Bates G. P. and Davies S. W. (2000) Non-apoptotic neurodegeneration in a transgenic mouse model of Huntington's disease. *Proc. Natl Acad. Sci. USA* **97**, 8093–8097.
- Yu Z. X., Li S. H., Evans J., Pillarsetti A., Li H. and Li X. J. (2003) Mutant huntingtin causes context-dependent neurodegeneration in mice with Huntington's disease. *J. Neurosci.* **23**, 2193–2202.
- Yuan J., Shaham S., Ledoux S., Ellis H. M. and Horvitz H. R. (1993) The *C. elegans* cell death gene *ced-3* encodes a protein similar to mammalian interleukin-1 $\beta$ -converting enzyme. *Cell* **75**, 641–652.
- Zha J., Harada H., Yang E., Jockel J. and Korsmeyer S. J. (1996) Serine phosphorylation of death agonist BAD in response to survival factor results in binding to 14-3-3 not BCL-X (L). *Cell* **87**, 619–628.
- Zou H., Henzel W. J., Liu X., Lutschg A. and Wang X. (1997) Apaf-1, a human protein homologous to *C. elegans* CED-4, participates in cytochrome c-dependent activation of caspase-3. *Cell* **90**, 405–413.